



# NATIONAL ADVISORY COMMITTEE FOR AERONAUTICS

TECHNICAL NOTE 3805

CALCULATION OF THE FORCES AND MOMENTS ON A  
SLENDER FUSELAGE AND VERTICAL FIN

PENETRATING LATERAL GUSTS

By John M. Eggleston

Langley Aeronautical Laboratory  
Langley Field, Va.



Washington

October 1956

AFMDC  
TECHNICAL LIBRARY  
OCT 20 1956



0066717

## NATIONAL ADVISORY COMMITTEE FOR AERONAUTICS

## TECHNICAL NOTE 3805

## CALCULATION OF THE FORCES AND MOMENTS ON A

## SLENDER FUSELAGE AND VERTICAL FIN

## PENETRATING LATERAL GUSTS

By John M. Eggleston

## SUMMARY

A theory is presented for calculating the variation with frequency of the lateral-force and yawing-moment coefficients due to sinusoidal side gusts passing over the profile of a simple fuselage-vertical-fin combination. The analysis is based on slender-body theory and is therefore applicable to both subsonic and supersonic airspeeds, provided the local flow angles between the profile and the airstream are small.

The force on any element along the length of a slender body (or flat plate) penetrating a gust is found to depend only on the body shape, the rate of change of body shape, and the local flow angle. However, when the same distribution of local flow angle is obtained by bending of the body, the force on the body depends both on these same functions and on the rate of change of local flow angle along the length of the body.

The present method of including the penetration effect of the fuselage and vertical tail in calculating airplane side force and yawing moment due to side gusts is believed to be more accurate than the use of a simple lag concept to account for the difference in time of penetration of the gust by the fuselage and the vertical fin.

## INTRODUCTION

In calculations involving the lateral forces and moments of an airplane striking a lateral gust, it has been usual to neglect the penetration effects and to estimate the forces and moments by considering the changes in flow angle to be constant over the configuration. For more accurate analysis of the motion of an airplane passing through gusts, it would be desirable to consider the penetration effect and the resulting phase variation of the forces and moments produced by components of the airplane which enter the gust at different times. An approximate method of accounting for such phase variations due to penetration was described

in reference 1, where the effectiveness of several autopilots in continuous atmospheric turbulence was analyzed. The approximation of reference 1 involved a linear time lag between the fuselage contribution, which acted at the center of gravity of the airplane, and the tail contribution, which acted at the quarter-chord point of the mean aerodynamic chord of the tail. A more refined method would be to define the pressure or lift distribution over the airplane due to a general gust distribution and to compute the forces and moments as the gust moves along the body. Such an analysis, based on slender-body theory, is presented in this report.

Slender-body theory was introduced into the calculation of the forces and moments of bodies of revolution and narrow pointed wings in steady flow by Munk (ref. 2) and Jones (ref. 3), respectively. Numerous discussions of the theory, its assumptions, physical concepts, and limitations may be found in the literature (see, for instance, the work of Miles in ref. 4) and will not be restated herein.

A generalized solution for a slender body or flat plate in unsteady flow was briefly outlined by Garrick in an appendix to reference 5. In his analysis, Garrick considered a slender airfoil of low aspect ratio performing arbitrary vertical translatory or bending motions while passing through an inviscid fluid at uniform velocity. Such an analysis lends itself to the inverse case of a rigid and nonrotating slender lifting surface passing at a uniform velocity through a transverse velocity fluctuation. By using a slender body of revolution and a flat pointed plate to represent the fuselage and vertical fin of an airplane, a solution for the forces and moments due to the penetration of arbitrary gusts may be found, and it is with this particular application that this paper is concerned.

The solution as derived herein is found to be in fairly simple form, and the frequency distributions of the lateral forces and moments are easily computed. This method of analysis is believed to be more accurate than methods which assume no penetration or which assume a linear lag due to penetration of an arbitrary gust by an airplane.

The theory and specific results of this paper may be identified with the so-called "Küssner effect." Küssner (ref. 6) derived an expression for the lift on a two-dimensional airfoil as it penetrates a sudden vertical-gust region without change in direction. The theory was extended to finite-span airfoils by Jones in reference 7 by means of thin-airfoil theory. In an appendix to reference 8 are given the indicial response and sinusoidal-gust response of several wing plan forms of very low aspect ratio. By properly relating the lifting surfaces analyzed in reference 8 to represent a fuselage-vertical-fin combination, results for the forces due to gusts may be obtained which are in agreement with those obtained in the present paper.

## SYMBOLS

b	wing span
h	pressure altitude
i	$\sqrt{-1}$
k	reduced-frequency parameter, $ax/U$
l	lift per unit length dx
$l_t$	tail length between airplane center of gravity and quarter-chord point of mean aerodynamic chord of vertical tail
p	static pressure
q	dynamic pressure
s(x)	semiwidth of profile along x (see sketch a)
$s_0, s_1$	dimensions measured from axis of symmetry (see sketch b)
S	wing area of airplane
t	time
U	free-stream velocity
v	transverse or side velocity
x	coordinate in direction of free stream
$x_0, x_1, x_2$	fuselage and fin coordinates (see sketch b)
z	coordinate normal to free-stream and transverse velocities
$\alpha_0$	trim angle of attack
$\beta$	lateral flow angle
$\rho$	density of air
$\mu_b$	airplane relative-density coefficient, $\frac{\text{Mass}}{\rho S b}$
$\omega$	circular frequency

$M_Z$  yawing moment about center of gravity

$F_Y$  side force

$C_n$  yawing-moment coefficient,  $M_Z/qSb$

$C_y$  side-force coefficient,  $F_Y/qS$

$C_L$  lift coefficient based on wing area

Subscript:

vt vertical tail

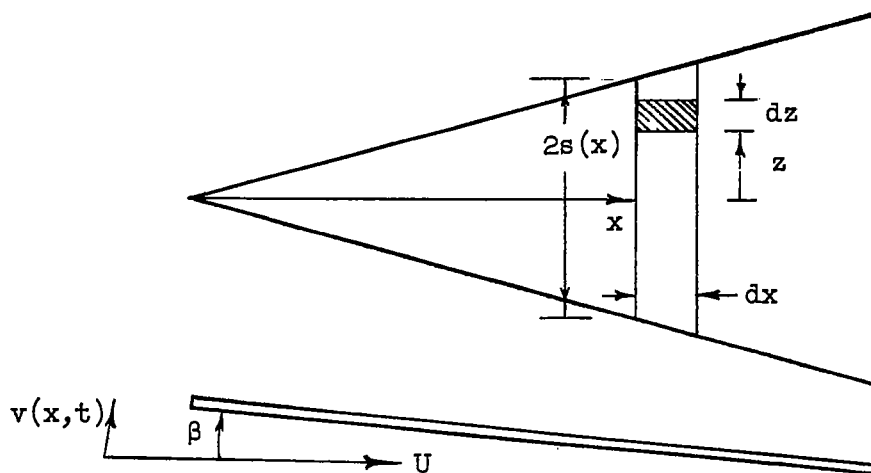
The absolute value of a complex quantity is denoted by  $| |$ .

### ANALYSIS

#### Lift on a Flat Pointed Plate or Slender Body

##### Due to Arbitrary Gusts

The following sketch shows a flat pointed plate of width  $2s$  inclined to the relative wind at an angle  $\beta$  and subjected to transverse velocity  $v(x,t)$ :



Sketch (a)

In reference 5, I. E. Garrick gives an expression for the lift per unit streamwise length of a flat plate of increasing area (but high fineness or low aspect ratio) subject to unsteady lift. In terms of  $v(x,t)$ , the expression for the lift per unit length of the flat plate shown in sketch (a) becomes:

$$\begin{aligned} l(x,t) &= \int p(x,z,t) dz \\ &= \pi \rho s^2(x) \frac{D}{Dt} v(x,t) + 2\pi \rho U s(x) \frac{ds}{dx} v(x,t) \end{aligned} \quad (1)$$

where the total derivative, within the approximations of slender-body theory, is a function of time and streamwise distance only:

$$\frac{D}{Dt} = \frac{\partial}{\partial t} + U \frac{\partial}{\partial x} \quad (2)$$

As derived, then, the lift per unit length is a function of body shape  $s(x)$ , the rate of change of body shape  $ds/dx$ , the local transverse velocity  $v$ , and the rate of change of the local velocity  $Dv/Dt$ . Where the lifting body is a nonrotating flat plate (or of such shape that it may be considered a flat plate in two-dimensional transverse flow) and the transverse velocity is considered to be some arbitrary gust distribution, an interesting simplification of equation (1) occurs. Since the gust at any instant of time is a summation of waves moving in the  $x$ -direction at a uniform velocity  $U$ , the general form of such a gust is defined by the relationship

$$v(x,t) = v(Ut-x) \quad (3)$$

It may be observed that this relationship is in the form of D'Alembert's classic solution to the general wave equation, which may be found in the literature. It is assumed herein that the gust velocity does not vary with time as it travels down the lifting body; as in D'Alembert's solution, it is assumed that the wave shape does not change with time as it moves along the coordinate  $x$ .

For a gust wave, then,

$$\begin{aligned} \frac{D}{Dt} v(x,t) &= \left( \frac{\partial}{\partial t} + U \frac{\partial}{\partial x} \right) v(Ut-x) \\ &= 0 \end{aligned}$$

and the first term of equation (1) is likewise zero. Thus, on the flat plate or slender body here considered, which is subjected to a gust whose velocity does not change with time while it is passing over the body, the lift per unit length is a function of the local flow angle only and not a function of the local rate of change of flow angle. Thus

$$l(x,t) = 2\pi\rho U s(x) \frac{ds}{dx} v(Ut-x) \quad (4)$$

Some general impressions may be drawn from this development. Since the gust velocity does not vary with time as it travels down the lifting body, only the shape of the body determines the change of momentum of the flow. If the body is an uncambered narrow plate of uniform width or a cylinder of uniform diameter, then on these sections of uniform area there is no change in momentum of the flow and no forces are developed. On the other hand, with a curved cylinder in a steady flow and a straight cylinder in a tunnel with wavy walls, the momentum of the crossflow would change with time and forces would be produced by the lifting surface. Where the nose sections of the lifting surfaces just discussed are pointed narrow airfoils or slender bodies of revolution, the lift is defined by equation (4).

#### Sinusoidal Gust Waves

Although any harmonic function having the form of equation (3) might be employed to represent a gust of arbitrary shape and magnitude, probably the simplest and most familiar harmonic function is the complex exponential. The gust velocity written in terms of this complex exponential is given by

$$v(x,t) = U\beta e^{i\frac{\omega}{U}(Ut-x)} \quad (5)$$

where it may be seen that, for a constant flow angle,  $v = U\beta$  and the expressions for lift in the preceding section reduce to the result of Jones (ref. 3) for a flat, uncambered airfoil in steady flow.

#### Side-Force and Yawing-Moment Coefficients

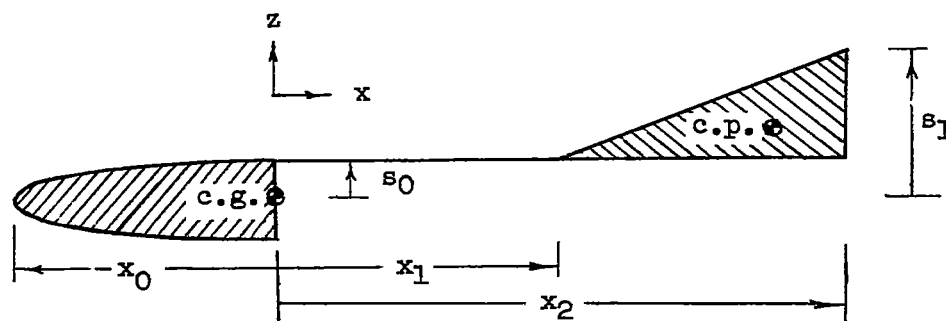
##### for a Simple Airplane Profile

Since the theory is applicable to airfoils with aspect ratio less than 1 and to slender bodies of revolution, a simplified version of the general shape of present-day aircraft must be employed. This simplified

fuselage—vertical-fin shape is hereinafter referred to as a profile. This profile, applicable to a large number of aircraft and also capable of treatment by the present theory, is used to compute the side force and yawing moment of a fuselage—vertical-tail combination.

The profile consists of a nose section of increasing area terminated at the center of gravity. That part of the fuselage downstream of the center of gravity will be neglected. Although the theory should apply to the contracting portion of an isolated fuselage, the flow separation effects and the interference due to a wing located in the vicinity of the center of gravity make it doubtful that the theory would apply in this region. The major contribution to the forces and moments downstream of the center of gravity will be considered to be derived from the vertical fin. Thus the two components of the simplified profile will be considered as independent lifting surfaces, any effects due to interference or cross flow being neglected.

In line with the foregoing discussion, a simple profile composed of a half-ellipse for the forward part of the fuselage and a right triangle for the vertical fin is employed. The major axis of the ellipse is aligned with the x-axis of the fuselage, and the center of the ellipse is coincident with the center of gravity of the airplane. The centroid of the right triangle is assumed to be coincident with the center of pressure of the vertical fin. This profile is shown in the following sketch:



Sketch (b)

The shape of the profile is defined analytically by

$$\left. \begin{aligned} s(x) &= \pm \frac{s_0}{x_0} \sqrt{x_0^2 - x^2} \\ \frac{ds}{dx} &= \mp \frac{s_0}{x_0} \frac{x}{\sqrt{x_0^2 - x^2}} \end{aligned} \right\} \quad (-x_0 \leq x \leq 0) \quad (6)$$

$$\left. \begin{aligned} s(x) - s_0 &= + \frac{s_1 - s_0}{x_2 - x_1} (x - x_1) \\ \frac{d[s(x) - s_0]}{dx} &= + \frac{s_1 - s_0}{x_2 - x_1} \end{aligned} \right\} \quad (x_1 \leq x \leq x_2) \quad (7)$$

The expression for lift per unit length of the profile is given by equation (4), and for a sinusoidal lateral gust defined by equation (5) the section lift becomes

$$\left. \begin{aligned} l(x,t) &= -2\pi\rho U^2 \beta \left(\frac{s_0}{x_0}\right)^2 x e^{i\frac{\omega}{U}(Ut-x)} & (-x_0 \leq x \leq 0) \\ l(x,t) &= \pi\rho U^2 \beta \left(\frac{s_1 - s_0}{x_2 - x_1}\right)^2 (x - x_1) e^{i\frac{\omega}{U}(Ut-x)} & (x_1 \leq x \leq x_2) \end{aligned} \right\} \quad (8)$$

Since the derivations of equations (1) and (4) were based on a symmetrical plan form, the contribution of the vertical tail is multiplied by a factor of one-half. In doing this, it is assumed that the horizontal tail or fuselage acts as an end plate on the half-delta vertical fin, and no other correction factor is necessary.

With the lateral gust referenced to the center of gravity,

$$\frac{v}{U}(t, x=0) = \beta e^{i\omega t} \quad (9)$$

The lift at each streamwise station due to a lateral gust of velocity  $\frac{v}{U}$  having a unit amplitude is given by the expressions

$$\left. \begin{aligned} l(x,\omega) &= -2\pi\rho U^2 \left(\frac{s_0}{x_0}\right)^2 x e^{-i\frac{\omega x}{U}} & (-x_0 \leq x \leq 0) \\ l(x,\omega) &= \pi\rho U^2 \left(\frac{s_1 - s_0}{x_2 - x_1}\right)^2 (x - x_1) e^{-i\frac{\omega x}{U}} & (x_1 \leq x \leq x_2) \end{aligned} \right\} \quad (10)$$

The side-force coefficient and yawing-moment coefficient due to a unit side gust are given by the integral over the  $x$  dimension of the profile:

$$\begin{aligned}
C_Y(\omega) &= \frac{1}{qS} \int_{\text{profile}} -l(x, \omega) dx \\
&= \frac{4\pi}{S} \left( \frac{s_0}{x_0} \right)^2 \int_{-x_0}^0 x e^{-i \frac{\omega x}{U}} dx - \frac{2\pi}{S} \left( \frac{s_1 - s_0}{x_2 - x_1} \right)^2 \int_{x_1}^{x_2} (x - x_1) e^{-i \frac{\omega x}{U}} dx \\
&= \frac{2\pi}{S} \left\{ \frac{2s_0^2}{k_0^2} \left[ 1 - (1 - ik_0) e^{ik_0} \right] + \left( \frac{s_1 - s_0}{k_2 - k_1} \right)^2 \left[ e^{-ik_1} - (1 - ik_1 + ik_2) e^{-ik_2} \right] \right\}
\end{aligned} \tag{11}$$

$$\begin{aligned}
C_n(\omega) &= \frac{1}{qSb} \int_{\text{profile}} x l(x, \omega) dx \\
&= \frac{-4\pi}{bS} \left( \frac{s_0}{x_0} \right)^2 \int_{-x_0}^0 x^2 e^{-i \frac{\omega x}{U}} dx + \frac{2\pi}{bS} \left( \frac{s_1 - s_0}{x_2 - x_1} \right) \int_{x_1}^{x_2} (x - x_1) x e^{-i \frac{\omega x}{U}} dx \\
&= \frac{2\pi}{bS} \left\{ \frac{-2x_0 s_0^2}{k_0^3} \left[ (2k_0 - ik_0^2 + i2) e^{ik_0} - i2 \right] + \frac{(x_2 - x_1)(s_1 - s_0)^2}{(k_2 - k_1)^3} \times \right. \\
&\quad \left. \left[ (2k_2 - k_1 - i2 - ik_1 k_2 + ik_2^2) e^{-ik_2} - (k_1 - i2) e^{-ik_1} \right] \right\}
\end{aligned} \tag{12}$$

where the notation

$$k_n = \frac{\omega x_n}{U} \quad (n = 0, 1, 2)$$

has been employed to refer to the reduced frequencies based on the physical dimensions of the profile shown in sketch (b). The minus sign appears in the expression for the side-force coefficient to agree with the generally accepted concept that a positive side gust (moving from starboard to port of the airplane) will produce a negative side force at zero frequency.

Equations (11) and (12) may be thought of as expressing the in- and out-of-phase components of the side force and yawing moment due to a unit side gust oscillating at some specified frequency. At zero frequency, equations (11) and (12) reduce to

$$C_{Y\beta} = C_Y(\omega=0) = -\frac{\pi}{S} \left[ 2s_0^2 + (s_1 - s_0)^2 \right] \quad (13)$$

$$C_{n\beta} = C_n(\omega=0) = \frac{2\pi}{3Sb} \left[ -2s_0^2 x_0 + (s_1 - s_0)^2 \left( x_2 + \frac{x_1}{2} \right) \right] \quad (14)$$

#### NUMERICAL EXAMPLE

In this section the profiles of three airplanes of various sizes, with configurations typical of some current designs, are used to illustrate the variations of side-force and yawing-moment coefficients due to unit sinusoidal side gusts of various frequencies. The profile dimensions used in the calculations, together with the flight conditions and the pertinent airplane dimensions on which the profiles are based, are given in table I.

In applying the theory of this paper to actual aircraft, certain practical considerations are involved. Since the expressions for the side force and yawing moment depend only on the configuration, it is recognized that wing-fuselage interference and other details of a particular design may have effects on directional stability which can be determined accurately only by wind-tunnel tests or flight measurements. Therefore, in order to adjust  $C_Y$  and  $C_n$  to the particular flight condition chosen, slight modifications in the profiles of the example airplanes were made until the theoretical coefficients at zero frequency were equal to values of  $C_{Y\beta}$  and  $C_{n\beta}$  for the example airplanes as determined by flight tests. This modification consisted in one case of a slight reduction in tail area and in another case of tripling the fuselage contribution to allow for two large engine nacelles and propellers. In general, whether these adjustments are required depends on the airplane configuration.

The variations with frequency of  $C_Y$  and  $C_n$  due to unit side gusts have been plotted in two forms for each of the three example airplanes: as in-phase and out-of-phase components, and also as the amplitudes and phase angles relating the unit side gust to the lateral coefficients. These variations are shown in figures 1 to 3 for a range of frequencies from 0 to 30 radians per second.

A second set of results is also shown in these figures in order to illustrate the difference between the profile theory of this paper and the so-called linearized-lag theory. This linearized-lag concept, as used in reference 1, for example, considers the wing-fuselage contribution to act at the center of gravity and the tail contribution to lag

behind the center of gravity as a function of the time required for the airplane to travel a distance equal to the tail length. Expressions generally used for this lag are:

$$C_{Y\beta}(\omega) \approx C_{Y\beta} \left[ 1 - i \frac{(C_{Y\beta})_{vt}}{C_{Y\beta}} \frac{l_t \omega}{U} \right]$$

$$C_{n\beta}(\omega) \approx C_{n\beta} \left[ 1 - i \frac{(C_{n\beta})_{vt}}{C_{n\beta}} \frac{l_t \omega}{U} \right]$$

This linear-lag concept has been applied to the three example airplanes, and the results are plotted in figures 1 to 3 in the form of dashed lines.

Noted on each figure is the natural frequency of the Dutch roll mode of motion of the example airplane. For the particular airplanes considered here, the difference in the parameters (side force and yawing moment) as obtained by the two methods is small up to approximately twice the Dutch roll frequency. At higher frequencies, however, the flow angle variation over the airplane has a greater effect, and the linearized-lag theory is no longer valid. This effect might be important on airplanes in which the Dutch roll frequency is higher in terms of fuselage lengths, that is, on airplanes of low density and high directional stability. It may be seen that, for an airplane of short tail length (airplane A, fig. 1), both theories are in fair agreement over the entire range of frequencies shown. However, for airplanes of longer tail lengths, the theories agree only at the lower frequencies. Although the variation with frequency of the side force is not generally as important as that of the yawing moment, it is interesting to note that the side-force linearized theory predicts an increasing amplitude with frequency, whereas the present profile theory agrees with physical reasoning that the amplitude should initially decrease with frequency.

It is believed, then, that although the frequency variation of these parameters might differ somewhat with the choice of profile shape, the trend obtained by considering the lift distribution over the profile gives results more nearly correct than a theory which does not consider this aspect. In cases where it is desirable to extend the lateral forces and moments to higher frequencies than the valid range of the linearized-lag theory, the present theory offers a refinement. Since both theories require only fairly simple calculations, the computation time should not be a factor for consideration.

## CONCLUDING REMARKS

A simple profile of a fuselage--vertical-fin combination has been used to derive a formula for the variation with frequency of the side force and yawing moment of an airplane penetrating a gust, and numerical examples of the results are presented.

In deriving the forces on any element along the length of a slender body or flat plate penetrating a gust, it was shown that the force depends only on body shape, rate of change of body shape, and the local flow angle. However, when the same distribution of local flow angle is obtained by bending of the body, the force on the body depends both on these same functions and on the rate of change of local flow angle along the length of the body.

The present method of including the penetration effect of the fuselage and vertical tail in calculating airplane side force and yawing moment due to side gusts is believed to be more accurate than the use of a simple lag concept to account for the difference in time of penetration of the gust by the fuselage and vertical fin.

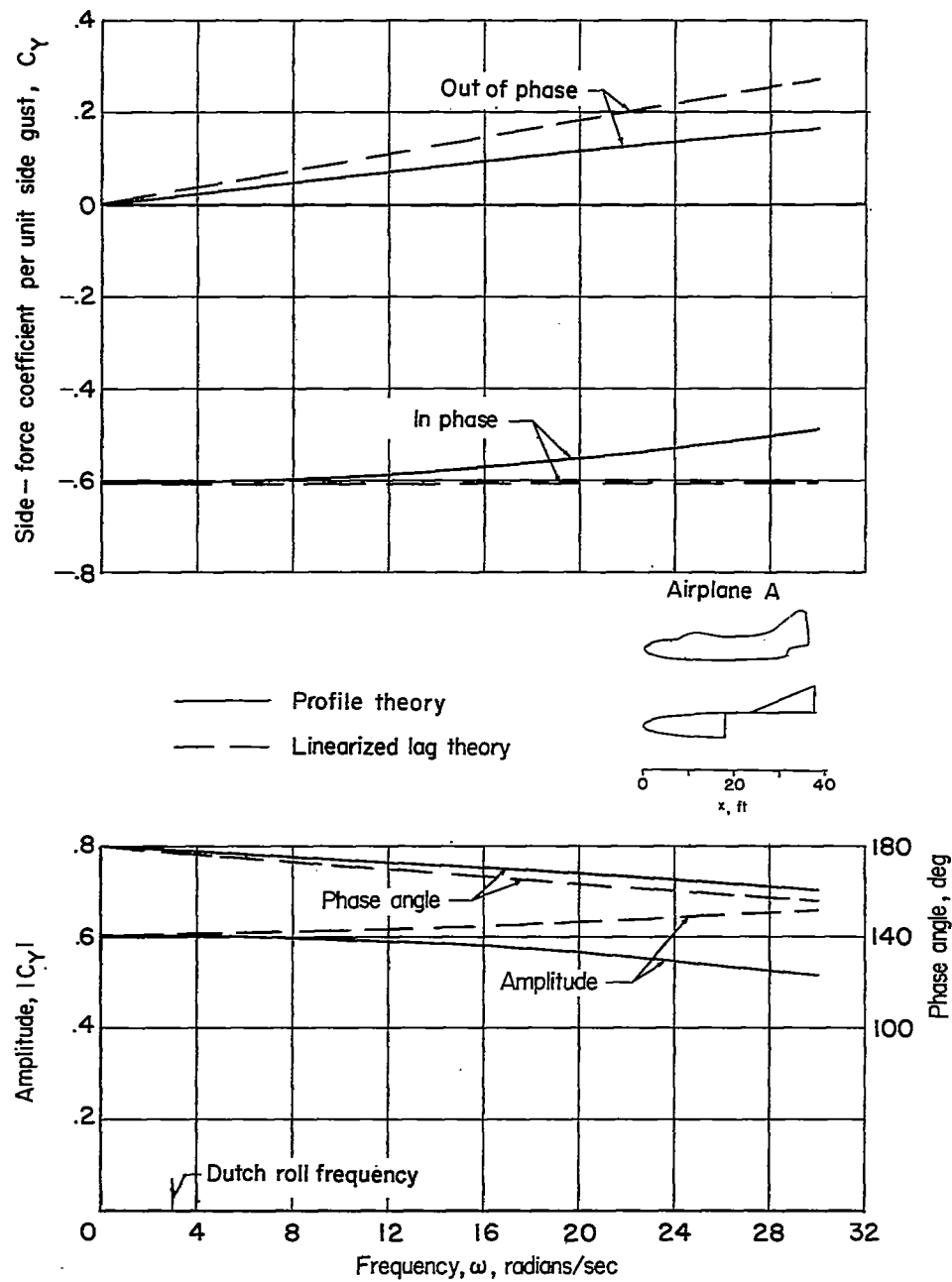
Langley Aeronautical Laboratory,  
National Advisory Committee for Aeronautics,  
Langley Field, Va., June 14, 1956.

## REFERENCES

1. Adams, James J., and Mathews, Charles W.: Theoretical Study of the Lateral Frequency Response to Gusts of a Fighter Airplane, Both With Controls Fixed and With Several Types of Autopilots. NACA TN 3603, 1956.
2. Munk, Max M.: The Aerodynamic Forces on Airship Hulls. NACA Rep. 184, 1924.
3. Jones, Robert T.: Properties of Low-Aspect-Ratio Pointed Wings at Speeds Below and Above the Speed of Sound. NACA Rep. 835, 1946. (Supersedes NACA TN 1032.)
4. Miles, John W.: On Non-Steady Motion of Slender Bodies. Aeronautical Quarterly, vol. II, pt. III, Nov. 1950, pp. 183-194.
5. Garrick, I. E.: Some Research on High-Speed Flutter. Third Anglo-American Aero. Conf., Sept. 4-7, 1951 (Brighton, England). R.A.S., 1952, pp. 419-446J.
6. Küssner, H. G.: Zusammenfassender Bericht über den instationären Auftrieb von Flügeln. Luftfahrtforschung, Bd. 13, Nr. 12, Dec. 20, 1936, pp. 410-424.
7. Jones, Robert T.: The Unsteady Lift of a Wing of Finite Aspect Ratio. NACA Rep. 681, 1940.
8. Drischler, Joseph A.: Approximate Indicial Lift Functions for Several Wings of Finite Span in Incompressible Flow As Obtained From Oscillatory Lift Coefficients. NACA TN 3639, 1956.

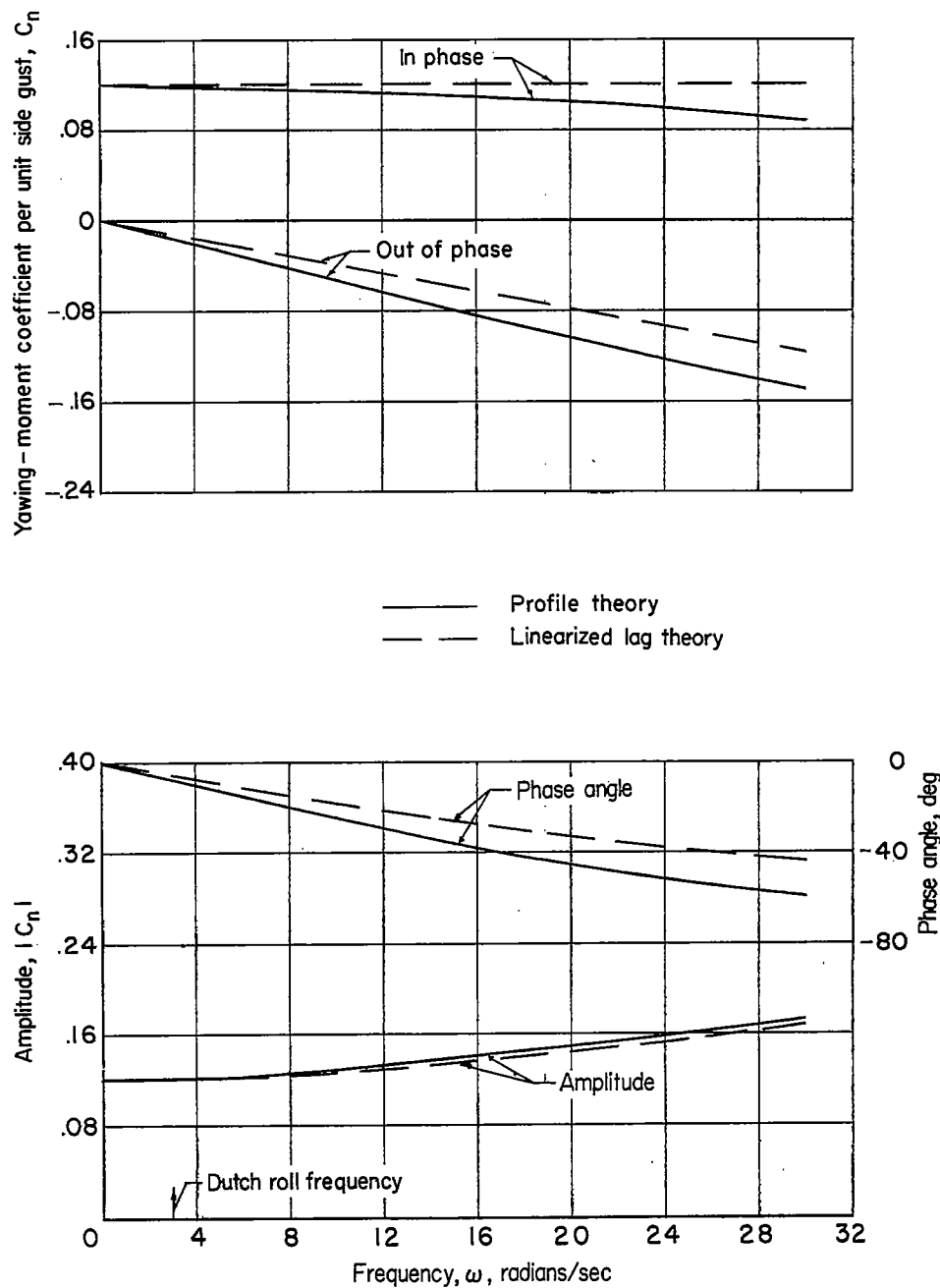
TABLE I  
FLIGHT CONDITIONS AND PHYSICAL CHARACTERISTICS  
OF EXAMPLE AIRPLANES

	Airplane A	Airplane B	Airplane C
Flight Conditions:			
$h$ , ft . . . . .	30,000	4,000	35,000
$U$ , ft/sec . . . . .	696	318	700
$\alpha_0$ , radians . . . . .	0.0586	0.0325	0.0823
$\mu_b$ . . . . .	50	10.9	31.83
$C_L$ . . . . .	0.242	0.177	0.443
Physical characteristics:			
$b$ , ft . . . . .	35.25	70	116
$S$ , sq ft . . . . .	250	540	1,428
$S_{vt}$ , sq ft . . . . .	55	71.35	230
$l_t$ , ft . . . . .	14.8	27.6	46.6
$x_0$ , ft . . . . .	18	15.25	48.5
$x_1$ , ft . . . . .	5.7	22.0	36.6
$s_0$ , ft . . . . .	2.7	3.0	5.3
$s_1$ , ft . . . . .	8.5	10.6	18.5



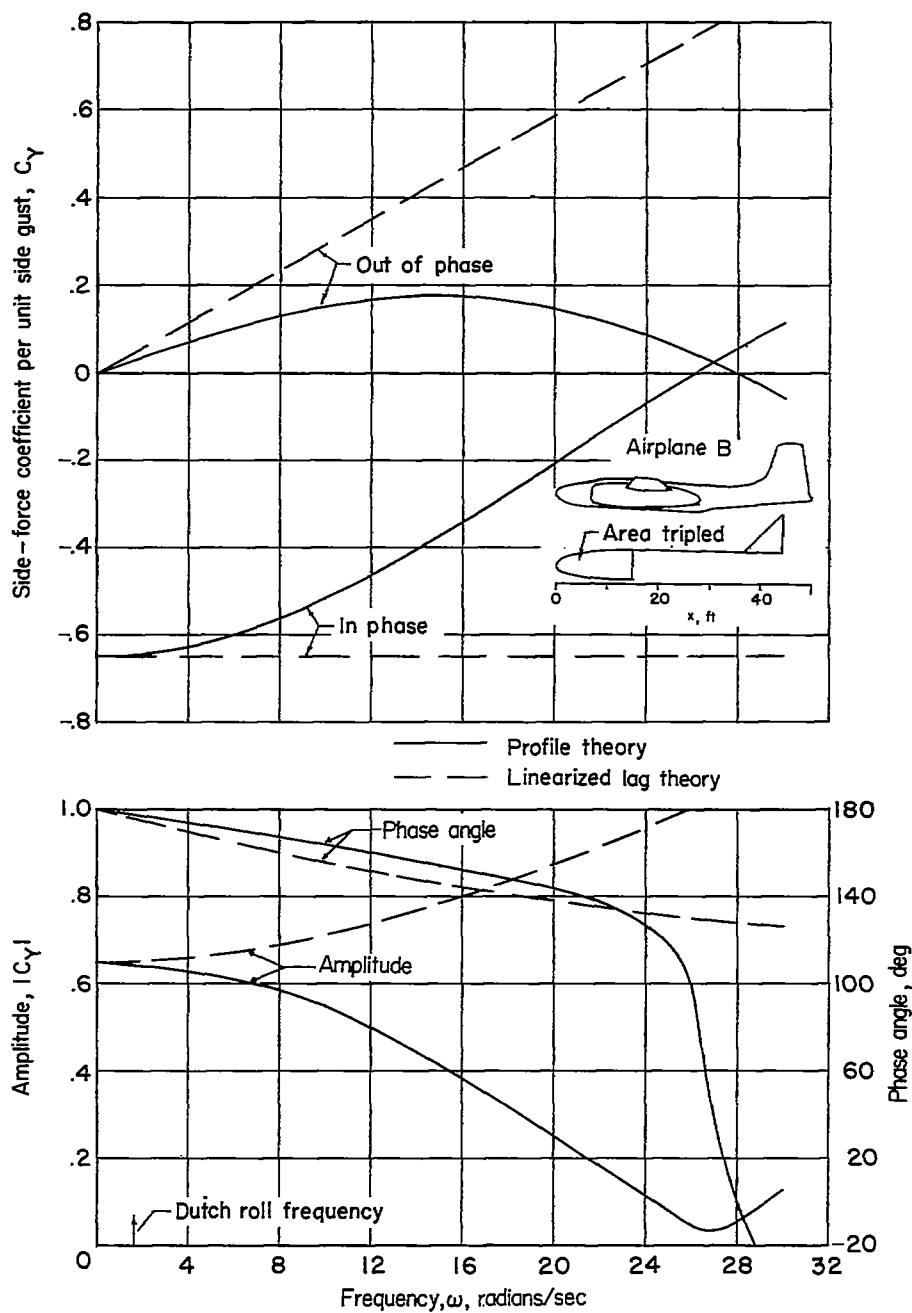
(a) Variation with frequency of side-force coefficient due to a unit side gust.

Figure 1.- Side-force and yawing-moment coefficients of airplane A as determined by profile and linearized theory.



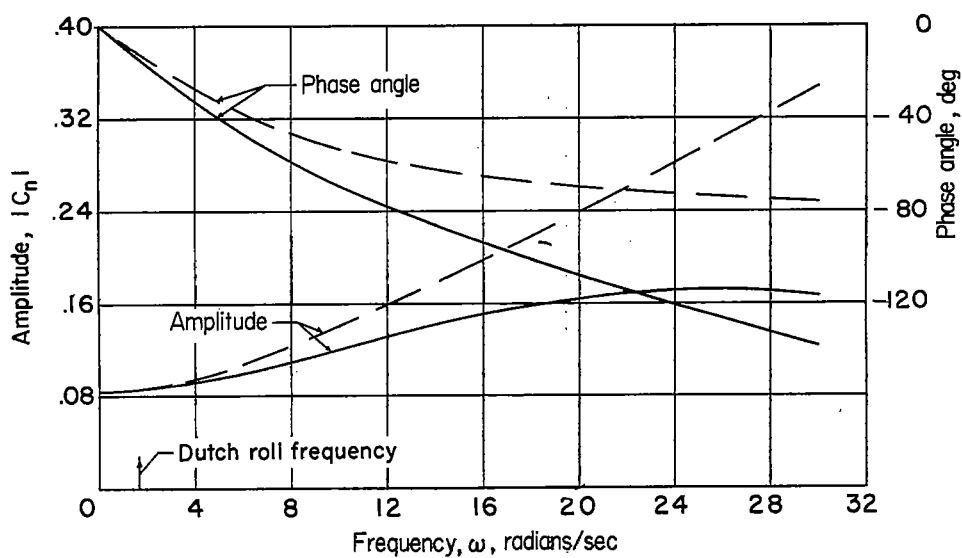
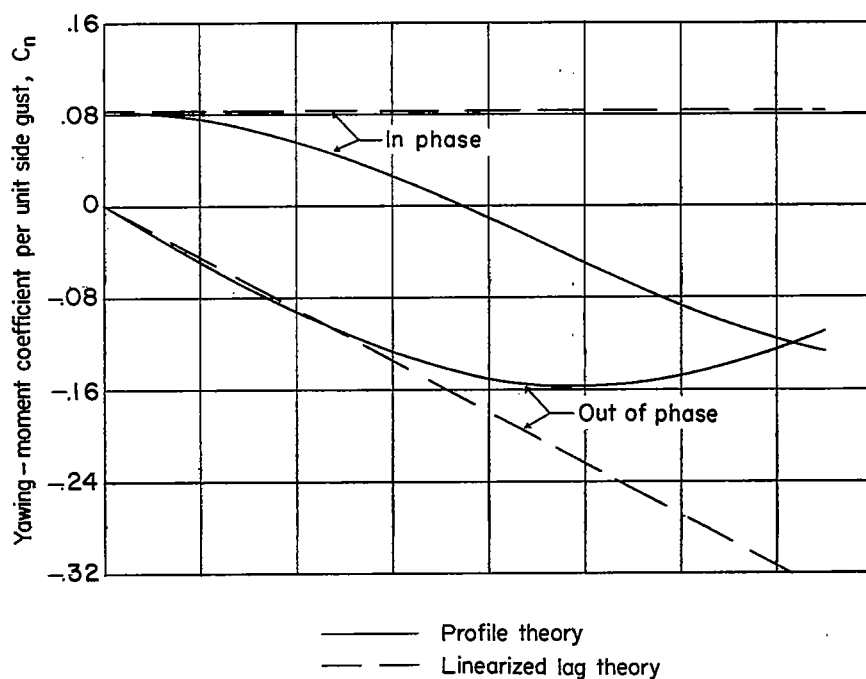
(b) Variation with frequency of yawing-moment coefficient due to a unit side gust.

Figure 1.- Concluded.



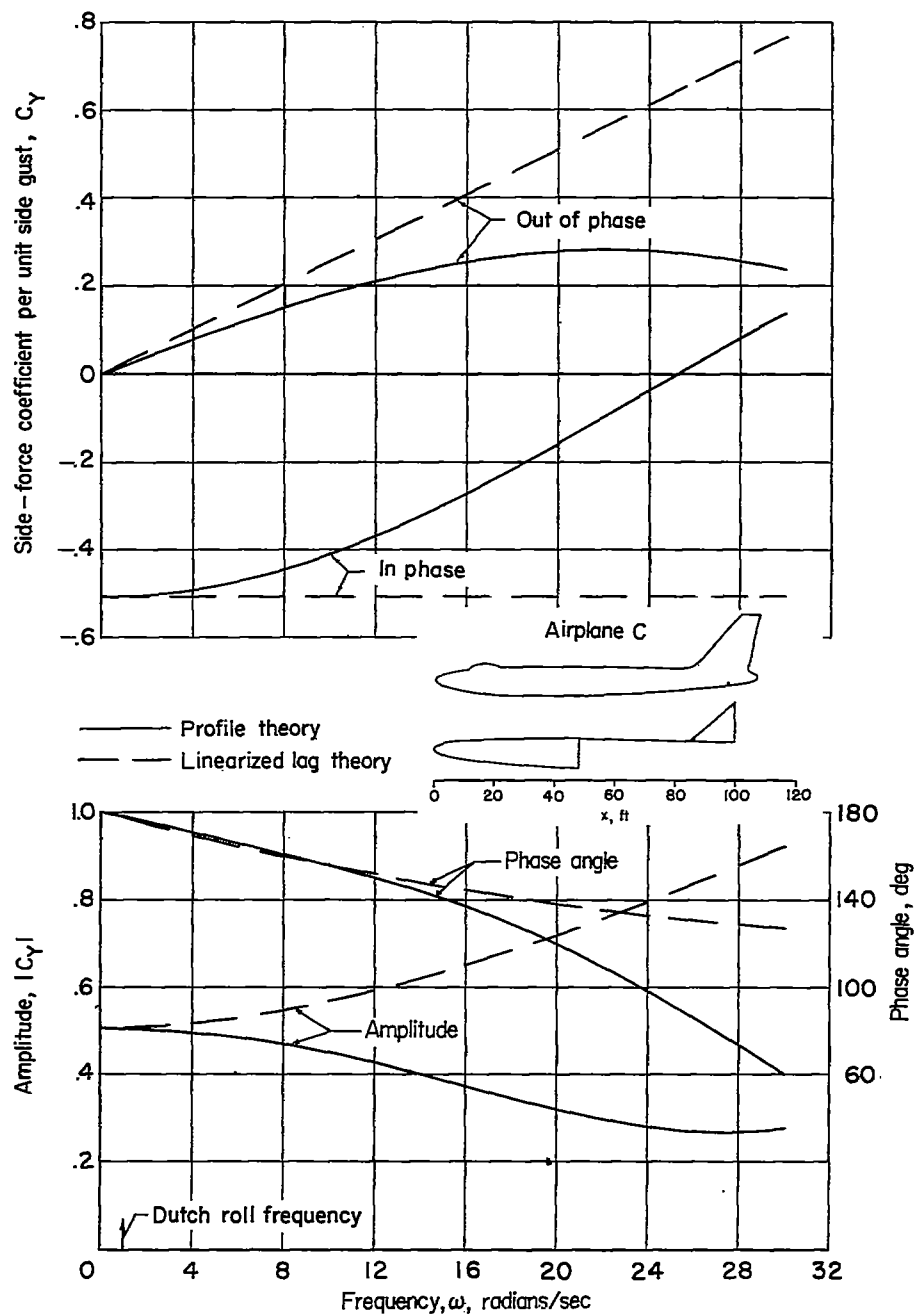
(a) Variation with frequency of side-force coefficient due to a unit side gust.

Figure 2.- Side-force and yawing-moment coefficients of airplane B as determined by profile and linearized theory.



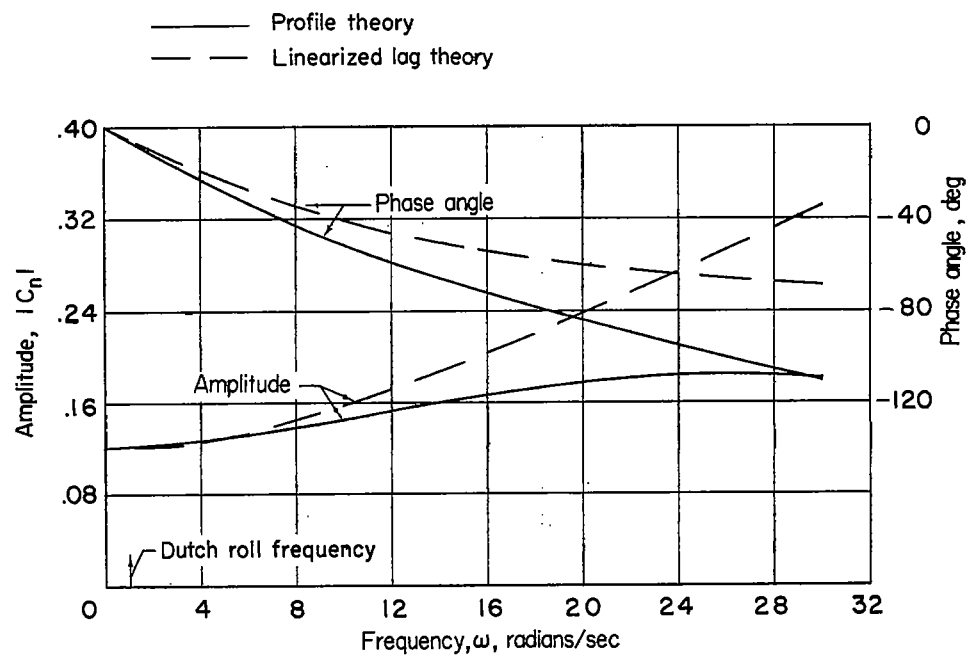
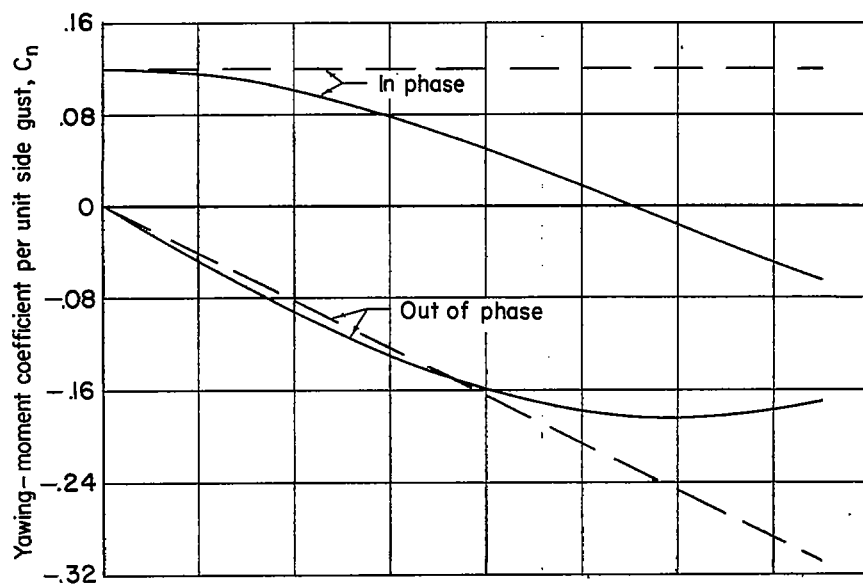
(b) Variation with frequency of yawing-moment coefficient due to a unit side gust.

Figure 2.- Concluded.



(a) Variation with frequency of side-force coefficient due to a unit side gust.

Figure 3.- Side-force and yawing-moment coefficients of airplane C as determined by profile and linearized theory.



(b) Variation with frequency of yawing-moment coefficient due to a unit side gust.

Figure 3.- Concluded.